Dual boundary element method for determining the reflection and transmission coefficients of oblique incident wave passing a thin submerged breakwater

K. H. Chen, J. T. Chen, C. R. Chou and C. Y. Yueh
Department of Harbor and River Engineering
National Taiwan Ocean University
Keelung, Taiwan

Abstract

In this paper, the dual integral formulation for the modified Helmholtz equation in solving the propagation of oblique incident wave passing a thin barrier (a degenerate boundary) is derived. All the improper integrals for the kernel functions in the dual integral equations are reformulated into regular integrals by integrating by parts and are calculated by means of the Gaussian quadrature rule. The jump properties for the single layer potential, double layer potential and their directional derivatives are examined and the potential distributions are shown. To demonstrate the validity of the present formulation, the transmission and reflection coefficients of oblique incident wave passing a thin rigid barrier are determined by the developed dual BEM program. Also, the results are obtained for the case of wave scattering by a rigid barrier with a zero thickness in a constant water depth and are compared with those of experiment and analytical solution using eigenfunction expansion method. Good agreement is made.
Key words: Key words: dual boundary element method, oblique incident wave, thin barrier, improper integral, singularity, hypersingularity, Gaussian quadrature, degenerate boundary, pseudo boundary, reflection coefficients, transmission coefficients

潛堤對斜向入射波消波影響之對偶邊界元素法分析

陳桂鴻　陳正宗　周宗仁　岳景雲

海洋大學河海工程學系, 基隆, 臺灣

摘要

本文以對偶邊界元素法 (DBEM) 分析潛堤承受 斜向與正向入射波所造成的消波影響。於分析時, 將奇異積分方程 (UT式) 及超奇異積分方程 (LM 式) 之 奇異積分與超奇異積分轉換成正規積分 。並分析單層勢能、雙層勢能與其方向導微之勢能的跳躍行爲, 而繪出其勢能分布圖, 進而發展一套解斜向與正向入射問題的對偶邊界元素程式。藉由此程式可得知流場的變化, 計算出反射係數 、穿透係數 。於極薄潛退化邊界問題時, 將 UT 式及 LM 式的相依方程組的互換, 解決解不唯一的問題。最後並以實例比較本法、解析解、有限元素法與實驗所得的數値結果, 驗證本法的可行性。
關鍵字: 斜向入射, 對偶邊界元素法, 奇異積分, 超奇異積分, 正規積分, 遠域幅射邊界條件, 反射係數, 穿透係數, 修正型霍姆赫斯方程, 退化邊界

1 Introduction

The dual formulation plays an important role in some problems, *e.g.*, corner problems [4], adaptive BEM [8], spurious eigenvalues of an interior problem [2], and fictitious frequencies of an exterior problem [1]. The present formulation totally has four kernel functions, which make possible a unified theory encompassing different schemes, various derivations and interpretations. For crack problems, a detailed derivation can be found in [7]. The order of singularity for the kernel in the normal derivative of the double layer potential is stronger than that of the Cauchy type kernel by one. The paradox of the nonintegrable kernel is introduced due to the illegal change of the integral and trace operators from the viewpoint of the dual integral formulation. Based on the theory of dual integral equations, the dual boundary element method has been implemented [5, 6]. The dual integral representation for the Laplace equation was proposed in [5] and a general purpose program, BEPO2D, was developed. Also, the program for crack problems has been developed by Hong and Chen [7] and Portela *et al.* [12]. For the Helmholtz equation, the dual formulation was developed by Chen and Chen [3]. In the same way, the acoustic problem of the Helmholtz equation with a screen was also solved successfully using the dual BEM program [3]. However, the dual BEM for the modified Helmholtz equation of a thin breakwater subject to oblique water wave was not constructed well to the authors' best knowledge.

Prediction of wave interactions has been studied previously by a number of authors for many kinds of configuration of a water barrier on the basis of linear wave diffraction theory [9]. Many analytical solutions have been developed on the basis of the eigenfunction expansion method [11] and the boundary element method [13]. Following the theory of dual integral equations and BEPO2D program developed by Chen and Hong [5, 6], the dual boundary element method has been modified to solve the water wave problem of normal incident water wave past a submerged thin barrier by Yueh and Tsaur [13]. The reflection and transmission of oblique incident water wave past a submerged barrier with a finite width were studied by using the conventional BEM under the linear wave theory [10]. In these references, the incident angle of wave, shape of barrier, barrier height, width and slope under various wave conditions have been considered. Nowadays, a thin barrier can be constructed to protect a harbor economically from the open sea. The primary function is to reduce the wave energy transmitted through it and to have the advantages of allowing water circulation, fish passage, providing economical protection. A suitable arrangement of a thin barrier may act as a good model for a breakwater. The effect of such an arrangement on incident wave can be studied by using the dual BEM, assuming linear theory for the thin breakwater.

In this paper, we will construct the dual integral formulation for solving the problems of oblique incident wave passing a "thin" water barrier, which is similar to the acoustic problem with a screen [3]. Thin water barrier and screen can be seen as degenerate boundaries. The governing equation considered here is the modified Helmholtz equation for oblique incident wave passing a thin water barrier instead of the Helmholtz equation for acoustic wave impinging on a screen. The rigid boundary condition of a thin barrier will be considered. All the improper integrals for the kernel functions (UT in the singular equation, LM in the hypersingular equation) encountered in the dual integral equations will be reformulated into regular integrals by integrating by parts and will be calculated by the Gaussian quadrature rule. The roles of hypersingular integral equation in the dual BEM for the problems with a degenerate boundary (thin barrier) will be examined. For the kernels in the dual formulation, we will extend our experiences of the dual formulation on the Laplace equation [6], Helmholtz equation [3] and the Navier equation [7] to the modified Helmholtz equation and will examine the potential properties of the four kernel functions. After discretizing the dual integral equations, a general purpose dual BEM program will be developed to solve the propagation of oblique incident wave passing a thin barrier with a zero thickness. The result will be compared with those of experiment and analytical solution by using the eigenfunction expansion method.

2 Dual integral formulation for the scattering wave problem with a thin water barrier (a degenerate boundary)

Consider a vertical thin barrier parallel to the z-axis as shown in Fig.1. A wave train with a frequency σ propagates towards the barrier with an angle θ in a constant water depth h. Assuming inviscid, incompressible fluid and irrotational flow, the wave field may be represented by the velocity potential $\Phi(x, y, z, t)$ which satisfies the Laplace equation as

$$\nabla^2 \Phi(x, y, z, t) = 0, \tag{1}$$

Based on the uniformity of the water depth in z-axis and the periodicity in time, the potential $\Phi(x, y, z, t)$ of fluid motion can be expressed as:

$$\Phi(x, y, z, t) = \phi(x, y)e^{i(\lambda z - \sigma t)} \tag{2}$$

where $\lambda = k\sin(\theta)$ and k is the wave number which satisfies the dispersion relation:

$$\sigma^2 = gk\tanh(kh), \tag{3}$$

in which g is the acceleration of gravity. The unknown function, $\phi(x, y)$, describes the fluctuation of the potential on the xy plane. Substition of Eqs.(2) into (1) yields the modified Helmholtz equation as follows:

$$\nabla^2\phi(x, y) - \lambda^2\phi(x, y) = 0, \ (x, y) \ in \ D, \tag{4}$$

where D is the domain of interest. The boundary conditions of the interested domain are summarized as:

1. The linearized free water surface boundary condition:

$$\frac{\partial\phi}{\partial y} - \frac{\sigma^2\phi}{g} = 0. \tag{5}$$

2. Seabed and breakwater boundary conditions:

$$\frac{\partial\phi}{\partial n} = 0., \tag{6}$$

where n is boundary normal vector.

3. Radiation condition at infinity:

$$\lim_{x\to\infty} x^{\frac{1}{2}}(\frac{\partial\phi}{\partial x} - ik\phi) = 0. \tag{7}$$

4. The fictitious boundary conditions on the interface:

For the infinite strip problem, the domain can be devided into three regions after introducing two pseudo-boundaries on both sides of the barrier, $x = \pm l$, as shown in Fig.1. The potential in the region I without energy loss can be expressed as:

$$\phi^{(1)}(x, y) = (e^{i\eta(x+l)} + Re^{-i\eta(x+l)})\frac{\cosh(k(h + y))}{\cosh(kh)} \tag{8}$$

where the superscript of ϕ denotes the region number, R is the reflection coefficient and $\eta = k\cos(\theta)$. The potential in the region III without energy loss can be expressed as:

$$\phi^{(3)}(x, y) = Te^{i\eta(x+l)}\frac{\cosh(k(h + y))}{\cosh(kh)}, \tag{9}$$

where T is the transmission coefficient. The fictitious boundary conditions on the interface are

$$\phi^{(1)}(-l, y) = \phi^{(2)}(-l, y) \tag{10}$$

$$\frac{\partial\phi^{(1)}}{\partial x}|_{x=-l} = \frac{\partial\phi^{(2)}}{\partial x}|_{x=-l} \tag{11}$$

$$\phi^{(3)}(l, y) = \phi^{(2)}(l, y) \tag{12}$$

$$\frac{\partial\phi^{(3)}}{\partial x}|_{x=l} = \frac{\partial\phi^{(2)}}{\partial x}|_{x=l} \tag{13}$$

According to Eqs.(8), (9), (10) and (12), we can derive the reflection and transmission coefficients as follows:

$$R = -1 + \frac{k}{n_0\sinh(kh)}\int_{-h}^{0}\phi^{(2)}(-l, y)\cosh(k(h + y))dy \tag{14}$$

$$T = \frac{k}{n_0\sinh(kh)}\int_{-h}^{0}\phi^{(2)}(l, y)\cosh(k(h + y))dy \tag{15}$$

where $n_0 = \frac{1}{2}(1 + \frac{2kh}{\sinh(2kh)})$.

The first equation of the dual boundary integral equations for the domain point can be derived from the Green's third identity [10]:

$$2\pi\phi(\tilde{x}) = \int_B T(\tilde{s},\tilde{x})\phi(\tilde{s})dB(\tilde{s}) - \int_B U(\tilde{s},\tilde{x})\frac{\partial\phi(\tilde{s})}{\partial n_{\tilde{s}}}dB(\tilde{s}),\ \tilde{x} \in D, \tag{16}$$

where $\tilde{x}$ is the field point ($\tilde{x} = (x,y)$), $\tilde{s}$ is the source point, and $T(\tilde{s},\tilde{x})$ is defined by

$$T(\tilde{s},\tilde{x}) \equiv \frac{\partial U(\tilde{s},\tilde{x})}{\partial n_{\tilde{s}}}, \tag{17}$$

in which $n_{\tilde{s}}$ denotes the normal vector at the boundary point $\tilde{s}$, and $U(\tilde{s},\tilde{x})$ is the fundamental solution which satisfies

$$\nabla^2 U(\tilde{x},\tilde{s}) - \lambda^2 U(\tilde{x},\tilde{s}) = \delta(\tilde{x}-\tilde{s}),\ \tilde{x} \in D. \tag{18}$$

In Eq.(18), $\delta(\tilde{x}-\tilde{s})$ is the Dirac-delta function. After taking normal derivative with respect to Eq.(16) for a thin barrier problem, the second equation of the dual boundary integral equations for the domain point is derived:

$$2\pi\frac{\partial\phi(\tilde{x})}{\partial n_{\tilde{x}}} = \int_B M(\tilde{s},\tilde{x})\phi(\tilde{s})dB(\tilde{s}) - \int_B L(\tilde{s},\tilde{x})\frac{\partial\phi(\tilde{s})}{\partial n_{\tilde{s}}}dB(\tilde{s}),\ \tilde{x} \in D, \tag{19}$$

where

$$L(\tilde{s},\tilde{x}) \equiv \frac{\partial U(\tilde{s},\tilde{x})}{\partial n_{\tilde{x}}}, \tag{20}$$

$$M(\tilde{s},\tilde{x}) \equiv \frac{\partial^2 U(\tilde{s},\tilde{x})}{\partial n_{\tilde{x}}\partial n_{\tilde{s}}}, \tag{21}$$

in which $n_{\tilde{x}}$ represents the normal vector of $\tilde{x}$. The explicit forms for the four kernel functions are shown in Table 1. By moving the field point $\tilde{x}$ in Eqs.(16) and (19) to the boundary, the dual boundary integral equations for the boundary point can be obtained as follows:

$$\pi\phi(\tilde{x}) = C.P.V.\int_B T(\tilde{s},\tilde{x})\phi(\tilde{s})dB(\tilde{s}) - R.P.V.\int_B U(\tilde{s},\tilde{x})\frac{\partial\phi(\tilde{s})}{\partial n_{\tilde{s}}}dB(\tilde{s}),\ \tilde{x} \in B, \tag{22}$$

$$\pi\frac{\partial\phi(\tilde{x})}{\partial n_{\tilde{x}}} = H.P.V.\int_B M(\tilde{s},\tilde{x})\phi(\tilde{s})dB(\tilde{s}) - C.P.V.\int_B L(\tilde{s},\tilde{x})\frac{\partial\phi(\tilde{s})}{\partial n_{\tilde{s}}}dB(\tilde{s}),\ \tilde{x} \in B, \tag{23}$$

where $R.P.V.$ is the Riemann principal value, $C.P.V.$ is the Cauchy principal value and $H.P.V.$ is the Hadamard (Mangler) principal value.

3 On the four kernel functions and their potentials

The four kernel functions, $U(\tilde{s},\tilde{x}), T(\tilde{s},\tilde{x}), L(\tilde{s},\tilde{x})$ and $M(\tilde{s},\tilde{x})$, in the dual integral equations have different orders of singularity when $\tilde{x}$ approaches $\tilde{s}$. The order of singularity and the symmetry properties for the four kernel functions and the continuous properties of the potentials across the boundary resulting from the four kernel functions are summarized in Table 1. In Table 1, not only the normal derivatives for the single and double layer potentials, but also the tangential derivatives are considered. For the regular elements, no special treatment is needed since the Gaussian quadrature rule can be directly employed. Without loss of generality, the four improper integrals for the singular elements obtained by using constant element scheme after coordinate transformation can be formulated into the following regular integrals:

(1) $U(\tilde{s},\tilde{x})$ kernel:

$$\begin{aligned} diag\,([U]) &= i\lim_{\epsilon\to 0}\int_{-0.5l}^{0.5l} D_0^{(1)}(\lambda\sqrt{s^2+\epsilon^2})ds \\ &= i\lim_{\epsilon\to 0}\{\int_{-0.5l}^{-\sqrt{\epsilon}} D_0^{(1)}(\lambda|s|)ds + \int_{-\sqrt{\epsilon}}^{\sqrt{\epsilon}}(-i)\ln(\lambda\sqrt{s^2+\epsilon^2})ds + \int_{\sqrt{\epsilon}}^{0.5l} D_0^{(1)}(\lambda s)ds\} \end{aligned}$$

$$\begin{aligned} &= i\lim_{\epsilon\to 0}\{\int_{-0.5l}^{-\sqrt{\epsilon}} D_0^{(1)}(\lambda|s|)ds + 0 + \int_{\sqrt{\epsilon}}^{0.5l} D_0^{(1)}(\lambda s)ds\} \\ &= i\{D_0^{(1)}(\frac{\lambda l}{2})l - \lambda\int_{-0.5l}^{0.5l}\{D_1^{(2)}(\lambda|s|)\,|s|\,ds\}, \end{aligned} \tag{24}$$

where $i^2 = -1$, $diag\,([U])$ denotes the diagonal element of the influence matrix $[U]$ (which will be elaborated on later in Eq.(28)), $D_0^{(1)}(\lambda s)$ is the first kind of the zeroth order modified Hankel function, l is the element length and the coordinate of the collocation point $\tilde{x}$ is $(0,0)$.
(2) $T(\tilde{s},\tilde{x})$ kernel:

$$\begin{aligned} diag\,([T]) &= i\lambda\lim_{\epsilon\to 0}\int_{-0.5l}^{0.5l} D_1^{(2)}(\lambda\sqrt{s^2+\epsilon^2})\frac{\epsilon}{\sqrt{s^2+\epsilon^2}}ds \\ &= i\lambda\lim_{\epsilon\to 0}\int_{-\sqrt[4]{\epsilon}}^{\sqrt[4]{\epsilon}}\frac{-i(1)}{\lambda\sqrt{s^2+\epsilon^2}}\frac{\epsilon}{\sqrt{s^2+\epsilon^2}}ds \\ &= \lim_{\epsilon\to 0}\arctan\frac{s}{\epsilon}\Big|_{-\sqrt[4]{\epsilon}}^{\sqrt[4]{\epsilon}} \\ &= \pi, \end{aligned} \tag{25}$$

where $D_1^{(2)}(\lambda s)$ is the second kind of the first order modified Hankel function and $[T]$ is the influence matrix (which will be elaborated on later in Eq.(29)).

(3) $L(\tilde{s},\tilde{x})$ kernel:

$$\begin{aligned} diag\,([L]) &= i\lambda\lim_{\epsilon\to 0}\int_{-0.5l}^{0.5l} D_1^{(2)}(\lambda\sqrt{s^2+\epsilon^2})\frac{-\epsilon}{\sqrt{s^2+\epsilon^2}}ds \\ &= \lim_{\epsilon\to 0} -i\lambda\int_{-\sqrt[4]{\epsilon}}^{\sqrt[4]{\epsilon}}\frac{-i(1)}{\lambda\sqrt{s^2+\epsilon^2}}\frac{\epsilon}{\sqrt{s^2+\epsilon^2}}ds \\ &= -\pi. \end{aligned} \tag{26}$$

where $[L]$ is the influence matrix (which will be elaborated on later in Eq.(30)).

(4) $M(\tilde{s},\tilde{x})$ kernel:

$$\begin{aligned} diag\,(M) &= -i\lambda\lim_{\epsilon\to 0}\int_{-0.5l}^{0.5l}\lambda\frac{D_2^{(1)}(\lambda\sqrt{s^2+\epsilon^2})}{s^2+\epsilon^2}(-\epsilon)(-\epsilon) + \frac{D_2^{(1)}(\lambda\sqrt{s^2+\epsilon^2})}{\sqrt{s^2+\epsilon^2}}ds \\ &= -i\lambda\{-2D_1^{(2)}(\frac{\lambda l}{2}) + \lambda[D_0^{(1)}(\frac{\lambda l}{2})l - \lambda\int_{-0.5l}^{0.5l} D_1^{(2)}(\lambda|s|)\;|s|\;ds\;]\}, \end{aligned} \tag{27}$$

where $D_2^{(1)}(\lambda s)$ is the first kind of the second order modified Hankel function and $[M]$ is the influence matrix (which will be elaborated on later in Eq.(31)). After the above manipulations, the improper integrals, including weak ($U(\tilde{s},\tilde{x})$), strong ($T(\tilde{s},\tilde{x}), L(\tilde{s},\tilde{x})$) and superstrong ($M(\tilde{s},\tilde{x})$) singularities, reduce to regular integrals and are calculated using the Gaussian quadrature rule.

The potentials of the six kernel functions, $U(\tilde{s},\tilde{x}), T(\tilde{s},\tilde{x}), L(\tilde{s},\tilde{x}), M(\tilde{s},\tilde{x}), L^t(\tilde{s},\tilde{x})$ and $M^t(\tilde{s},\tilde{x})$ in Table 1, induced by the constant singularity source distributed along the boundary from $\tilde{s} = (-0.5,0)$ to $\tilde{s} = (0.5,0)$ are shown in Figs.2 and 4 for different values of $\lambda = 0.01$ and 10, respectively. The behavior of the single layer potential ($U(\tilde{s},\tilde{x})$ kernel), the double layer potential ($T(\tilde{s},\tilde{x})$ kernel), the normal derivative of the single layer potential ($L^n(\tilde{s},\tilde{x})$ kernel), the normal derivative of the double layer potential ($M^n(\tilde{s},\tilde{x})$ kernel), the tangential derivative of the single layer potential ($L^t(\tilde{s},\tilde{x})$ kernel) and the tangential derivative of the double layer potential ($M^t(\tilde{s},\tilde{x})$ kernel) are all shown in the figures where only real part is considered. It is found the asymptotic behavior of the real part of the kernels for the modified Helmholtz equation in Figs.2 for $\lambda = 0.01$ are similar to that of the Laplace equation in [5, 6] as expected. The continuous behaviors of the single layer potential ($U(\tilde{s},\tilde{x})$ kernel) and the normal derivative of the double layer potential ($M(\tilde{s},\tilde{x})$ kernel) are displayed in this figures. The jump behaviors across the boundary connected from $\tilde{s} = (-0.5,0)$ to $\tilde{s} = (0.5,0)$ can be observed for the double layer potential ($T(\tilde{s},\tilde{x})$ kernel) and the normal derivative of the single layer potential ($L(\tilde{s},\tilde{x})$ kernel). Also, the dipole and quadrapole source structures are found. Based on the singular solutions, the strength of the singularity can be determined by satisfying the boundary conditions.

4 Dual boundary element method for a thin barrier

By discretizing Eqs(22) and (23) using boundary elements, we can obtain the transcendental equation as follows:

$$[\bar{T}_{ij}(\lambda)]\{\phi_j\} = [U_{ij}(\lambda)]\{(\frac{\partial \phi}{\partial n})_j\},$$

$$[M_{ij}(\lambda)]\{\phi_j\} = [\bar{L}_{ij}(\lambda)]\{(\frac{\partial \phi}{\partial n})_j\},$$

where the elements of the four influence matrices are

$$U_{ij}(\lambda) = R.P.V. \int_{B_j} U(\tilde{s}_j, \tilde{x}_i) dB(\tilde{s}_j), \tag{28}$$

$$\bar{T}_{ij}(\lambda) = -\pi\delta_{ij} + C.P.V. \int_{B_j} T(\tilde{s}_j, \tilde{x}_i) dB(\tilde{s}_j), \tag{29}$$

$$\bar{L}_{ij}(\lambda) = \pi\delta_{ij} + C.P.V. \int_{B_j} L(\tilde{s}_j, \tilde{x}_i) dB(\tilde{s}_j), \tag{30}$$

$$M_{ij}(\lambda) = H.P.V. \int_{B_j} M(\tilde{s}_j, \tilde{x}_i) dB(\tilde{s}_j), \tag{31}$$

in which λ is imbedded in the elements of each matrix, $\tilde{x}_i$ is the i^{th} collection point, $dB(\tilde{s}_j)$ is the j^{th} integration element and B_j denotes the j^{th} boundary element. After combining the dual equations on the degenerate boundary when $\tilde{x}$ collocates on C^+ or C^-, the singular system of the four influence matrix is desingularized. Since either one of the two equations, UT or LM, for the outer boundary S can be selected, two alternative approaches, $UT + LM$ and $LM + UT$ in Fig.4, are proposed.

5 Illustrative examples

To demonstrate the validity of the dual integral formulation, The example is given as follows:
An example given by Losada *et al.* [11] is considered. The boundary mesh is shown in Fig.5. The submergence ratio ($\frac{d}{h}$) is 0.7 and the thickness of the barrier is modeled as zero thickness, *i.e.*, the boundary of barrier is degenerate. Based on the dual formulation, the reflection and transmission coefficients are plotted against kh for $\theta = 0^o$ in Fig.6. The results were compared with the eigenfunction expansion method by Losada *et al.* [11] and the experimental data by Ogilvie *et al.* [11]. Good agreement among the three solutions is made. The reflection and transmission coefficients are plotted versus the angle of incidence (θ) for $kh = 2.136$ as shown in Fig.7. The two solutions, $UT + LM$ and $LM + UT$ approaches, match well with the eigenfunction solution.

In order to study the sensitivity of barrier thickness, the nonzero thickness of $5\,m$ and $10\,m$ are also considered. The comparisons of the reflection and transmission coefficients of the three cases are plotted against kh for $\theta = 0^o$ as shown in Fig.8. The comparisons of the reflection and transmission coefficients for the three cases are plotted against θ for $kh = 2.136$ as shown in Fig.9. Further experiments will be conducted to verify the phenomenon in the future.

6 Conclusions

The dual integral formulation for the boundary value problem of the modified Helmholtz equation in solving the propagation of oblique incident wave passing a thin barrier (a degenerate boundary) has been derived in this paper. The properties of the potentials resulting from the four kernel functions in the dual integral equations have been examined, and their potential distributions have also been given. A general purpose dual BEM program has been developed to solve for the water scattering problem passing a barrier. The example for the problem with a zero thickness barrier has been successfully solved using the proposed dual BEM, and the results were compared well with those obtained using analytical solution and experiments.

Acknowledgement

Financial support from the National Science Council, Grant No. NSC-89-2211-E-019-022, for National Taiwan Ocean University is gratefully acknowledged.

References

[1] Chen J. T., Chen C. T., Chen K. H. and Chen I. L., On fictitious frequencies using dual bem for non-uniform radiation problems of a cylinder, *Mechanics Research Communications*, 2000, **27**(6), 685-690.

[2] Chen J. T., Kuo S. R. and Chen K. H., A nonsingular formulation for the Helmholtz eigenproblems of a circular domain, *Journal of Chinese Institute of Engineers*, 1999, **22**(6), 729-739.

[3] Chen J. T., Chen K. H., Dual integral formulation for determining the acoustic modes of a two-dimensional cavity with a degenerate boundary, *Engineering Analysis with Boundary Elements*, 1998, **21**, 105-116.

[4] Chen J. T. and Hong H.-K., Dual boundary integral equations at a corner using contour approach around singularity, *Advances in Engineering Software*, 1994, **21**(3), 169-178.

[5] Chen J. T. and Hong H.-K., Review of dual integral representations with Emphasis on hypersingular integrals and divergent series, it Transations of ASME, *Applied Mechanics Review*, **52** **(1)**, 17-33, 1999.

[6] Chen, J. T. and Hong, H.-K., *Boundary element method*, Second Edition, New World Press, Taipei, Taiwan, 1992 (in Chinese).

[7] Hong H.-K. and Chen J. T., Derivations of integral equations of elasticity, *Journal of Engineering Mechanics (ASCE)*, 1988, **114**(6), 1028-1044.

[8] Liang M. T., Chen J. T., Yang S. S., Error estimation for boundary element method, *Engineering Analysis with Boundary Elements*, 1999, **23**, 257-265.

[9] Liu P. L. F. and Wu J., Transmission through submerged apertures, *Journal Waterway Port Coast and Ocean Engineering (ASCE)*, 1987, **113**(6), 660-671.

[10] Liu P. L. F. and Abbaspour Madjid, An integral equation method for the diffraction of oblique wave by an infinite cylinder, *International Journal for Numerical Methods in Engineering*, 1982, **18**, 1497-1504.

[11] Losada Indigo J., Losada Miguel A. and Roldan J., Propagation of oblique incident waves past rigid vertical thin barriers, *Applied Ocean Research*, 1992, **14**, 191-199.

[12] Portela A., Aliabadi M. H. and Rooke D. P., The dual boundary element method : effective implementation for crack problems, *International Journal for Numerical Methods in Engineering*, 1992, **33**, 1269-1287.

[13] Yueh Ching Yun and Tsaur Deng How, Wave scattering by submerged vertical plate-type breakwater using composite BEM, *Coastal Engineering Journal*, 1999, **41**(1), 65-83.

Table 1 The properties of the kernel functions for the modified Helmholtz equation.

Kernel function $K(\tilde{s},\tilde{x})$	$U(\tilde{s},\tilde{x})$	$T(\tilde{s},\tilde{x})$	$L(\tilde{s},\tilde{x})$	$M(\tilde{s},\tilde{x})$	$L^t(\tilde{s},\tilde{x})$	$M^t(\tilde{s},\tilde{x})$
Explicit forms	$U(\mathbf{s},\mathbf{x}) = iD_0^{(1)}(\lambda r)$	$T(\mathbf{s},\mathbf{x}) = -i\lambda D_1^{(2)}(\lambda r)\frac{y_i n_i}{r}$	$L(\mathbf{s},\mathbf{x}) = i\lambda D_1^{(2)}(\lambda r)\frac{y_i \bar{n}_i}{r}$	$M(\mathbf{s},\mathbf{x}) = -i\lambda\{\lambda\frac{D_2^{(1)}(\lambda r)}{r^2} y_i y_j n_i \bar{n}_j + \frac{D_1^{(2)}(\lambda r)}{r} n_i \bar{n}_i\}$	$L(\mathbf{s},\mathbf{x}) = i\lambda D_1^{(2)}(\lambda r)\frac{y_i \bar{t}_i}{r}$	$M(\mathbf{s},\mathbf{x}) = -i\lambda\{\lambda\frac{D_2^{(1)}(\lambda r)}{r^2} y_i y_j t_i \bar{t}_j + \frac{D_1^{(2)}(\lambda r)}{r} t_i \bar{t}_i\}$
Order of singularity	O(*1/ln r*) weak	O(*1/r*) strong	O(*1/r*) strong	$O(1/r^2)$ hypersingular	O(*1/r*) strong	$O(1/r^2)$ hypersingular
Symmetry	$U(\tilde{x},\tilde{s})$	$L(\tilde{x},\tilde{s})$	$T(\tilde{x},\tilde{s})$	$M(\tilde{x},\tilde{s})$	$M^t(\tilde{s},\tilde{x})$	$L^t(\tilde{s},\tilde{x})$
Density function $\upsilon(\tilde{s})$	$\frac{\partial\phi}{\partial n}$	ϕ	$\frac{\partial\phi}{\partial n}$	ϕ	$\frac{\partial\phi}{\partial t}$	ϕ
Potential type	single layer	double layer	normal derivative of single layer	normal derivative of double layer	tangential derivative of single layer	tangential derivative of double layer
$\int K(\tilde{s},\tilde{x})\upsilon(\tilde{s})dB(\tilde{s})$ continuity across boundary	continuous	discontinuous	discontinuous	Psuedo-continuous	continuous	discontinuous
Jump value	No jump	$2\pi\phi$	$2\pi\frac{\partial\phi}{\partial n}$	No jump	No jump	$2\pi\frac{\partial\phi}{\partial t}$
Principal value	Riemann	Cauchy	Cauchy	Hadamard	Cauchy	Hadamard

where $D_n^{(1)}(\lambda r)$ is the first kind of *n-th* order modified Hankel function, $\bar{n}_i$ and $\bar{t}_i$ denote the *ith* component of normal and tangent on $\tilde{x}$, respectively.

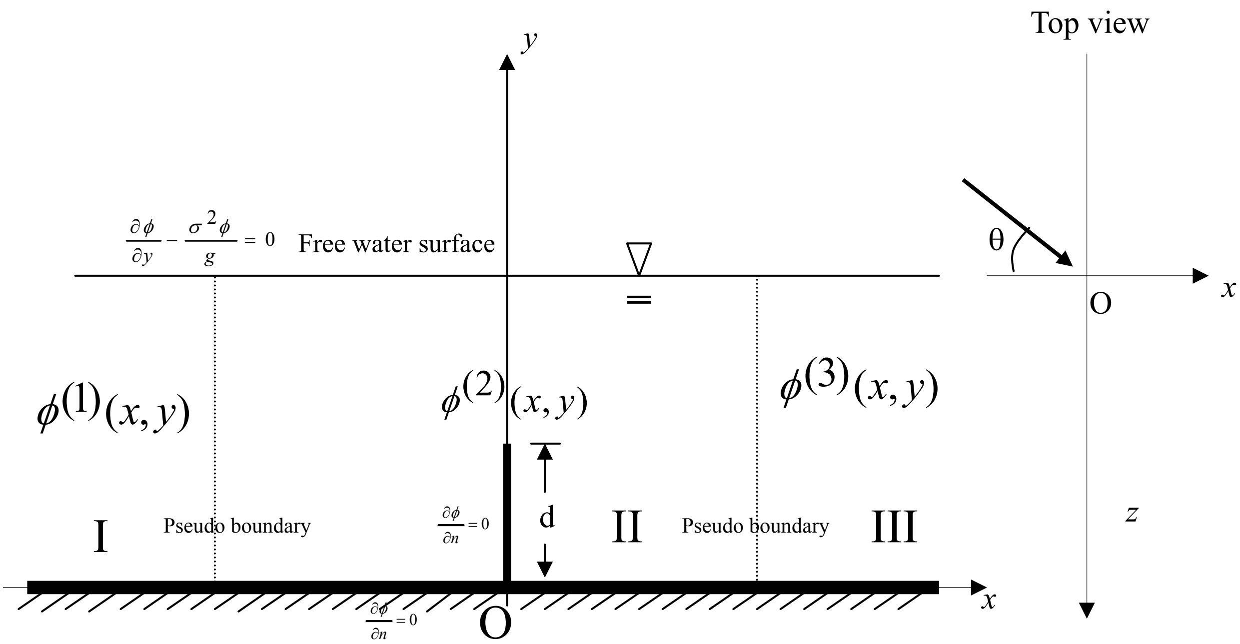

Fig1. Definition sketch of the water scattering problem of

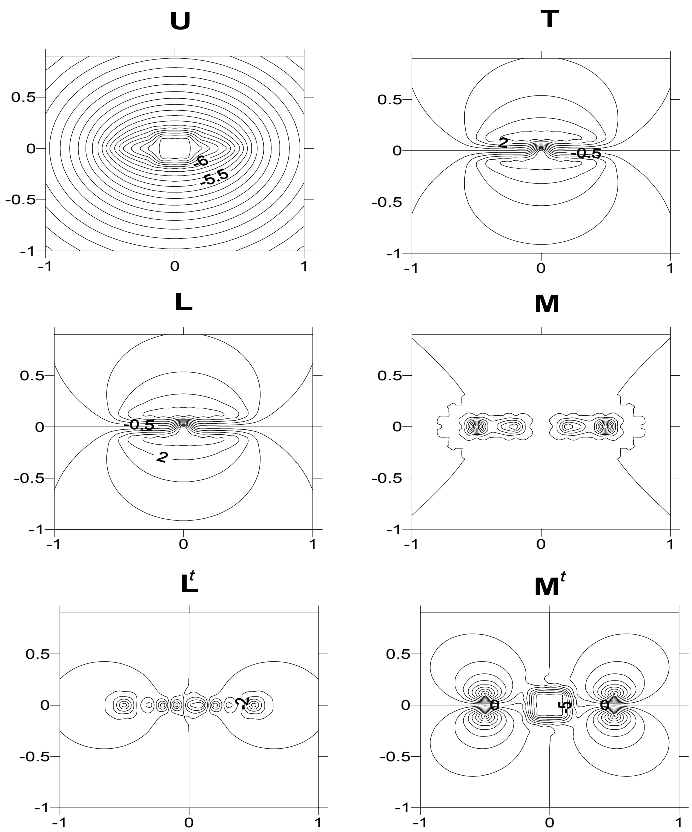

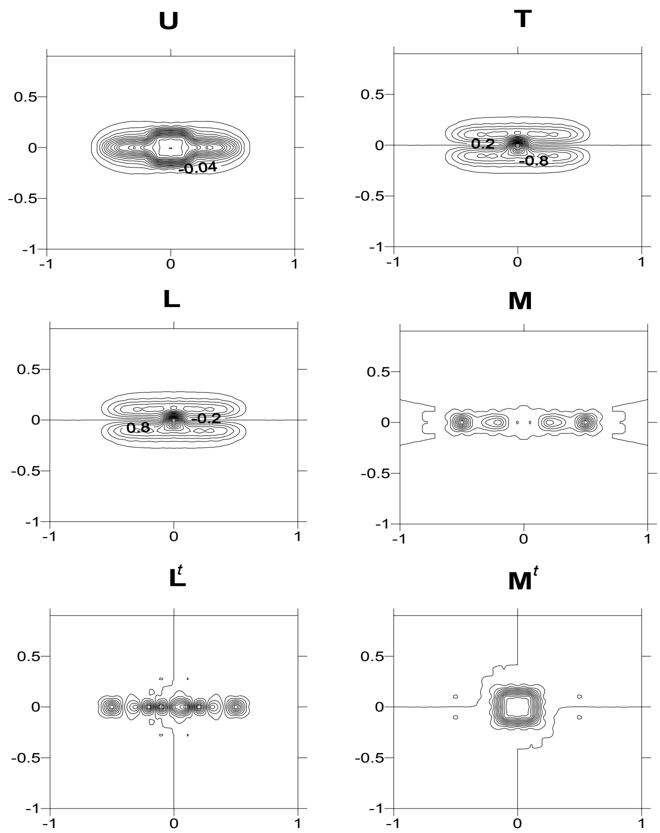

Fig.2 Contours of the real-part potentials resulting from the six kernel functions for the case of λ=*0.01*.

Fig.3 Contours of the real-part potentials resulting from the six kernel functions for the case of λ=*10*.

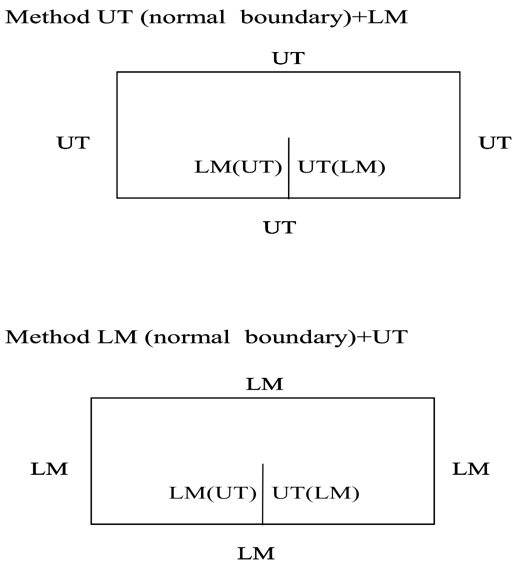

Fig.4 Two alternative approaches.

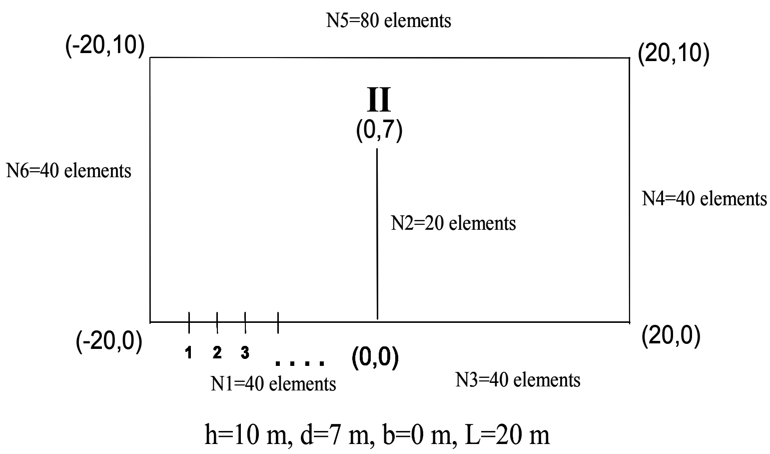

Fig.5 The boundary element mesh.

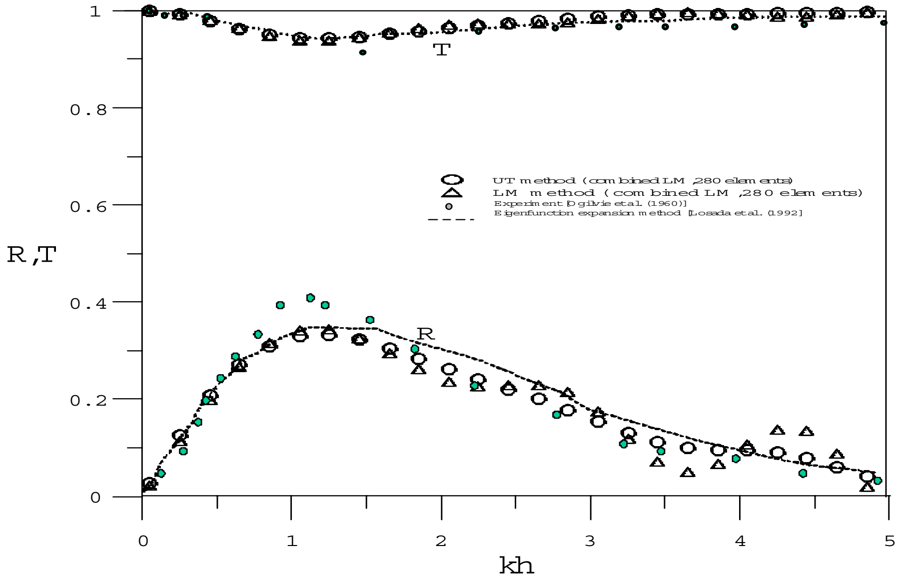

Fig.6 The reflection and transmission coefficients versus *kh* for $\theta = 0^o$.

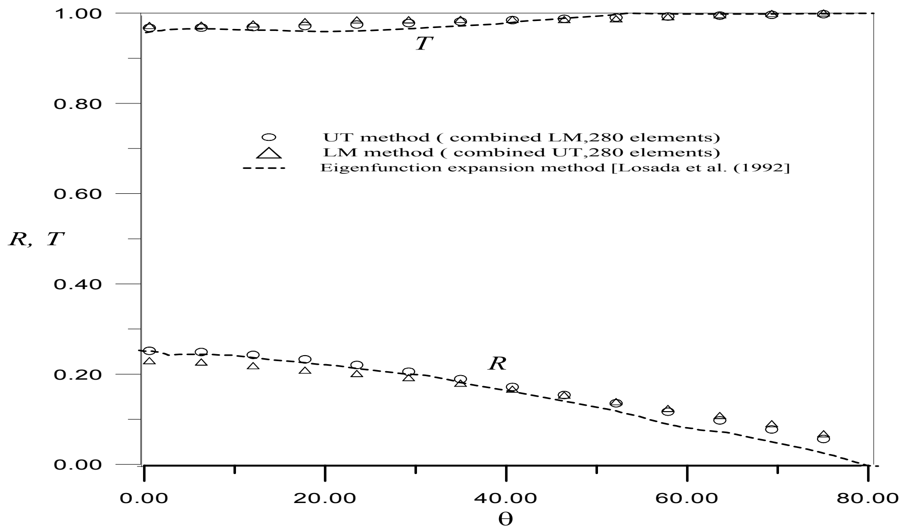

Fig.7 The reflection and transmission coefficients versus θ for *kh=2.136.*

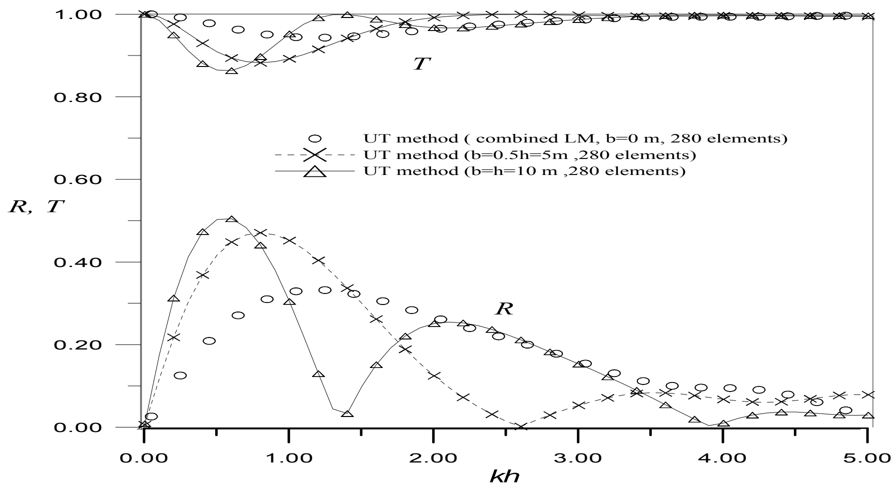

Fig.8 The comparisons of the reflection and transmission coefficients versus *kh* for the three cases, $\theta = 0^o$.

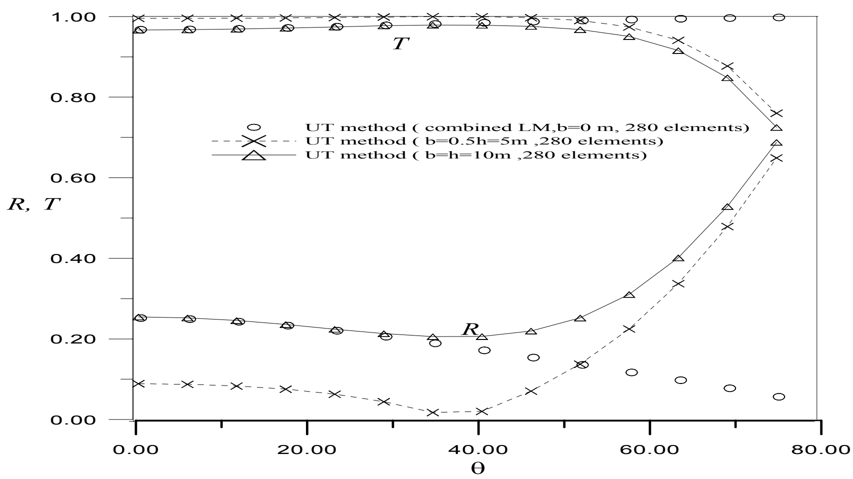

Fig.9 The comparisons of the reflection and transmission coefficients versus θ for the three cases, *kh=2.136.*

潛堤對斜向入射波消波影響之對偶邊界元素法分析

陳桂鴻　陳正宗　周宗仁　岳景雲

海洋大學河海工程學系，基隆，臺灣

摘要

本文以對偶邊界元素法(DBEM)分析潛堤承受斜向與正向入射波所造成的消波影響。於分析時，將奇異積分方程(UT 式)及超奇異積分方程(LM 式)之奇異積分與超奇異積分轉換成正規積分。並分析單層勢能、雙層勢能與其方向導微之勢能的跳躍行為，而繪出其勢能分布圖，進而發展一套解斜向與正向入射問題的對偶邊界元素程式。藉由此程式可得知流場的變化，計算出反射係數、穿透係數。於極薄潛退化邊界問題時，將 UT 式及 LM 式的相依方程組的互換，解決解不唯一的問題。最後並以實例比較本法、解析解、有限元素法與實驗所得的數值結果，驗證本法的可行性。

關鍵字：斜向入射，對偶邊界元素法，奇異積分，超奇異積分，正規積分，遠域幅射邊界條件，反射係數，穿透係數，修正型霍姆赫斯方程，退化邊界